An Accurate Position Estimation Method for Switched Reluctance Motor Drive

Debiprasad Panda , V.Ramanarayanan
Department of Electrical Engineering
Indian Institute of Science
Bangalore-560012
email: dpanda,vram@ee.iisc.ernet.in

Abstract: *In this paper a low-cost sensorless control strategy of SR motor is proposed. The static flux-linkage characteristics of the motor are used for estimating the position. A number of discrepancies between the static and the dynamic characteristics of the motor are explained. In this paper the issues regarding eddy effects and mutual inductances in both static and dynamic conditions, and their influence on position estimation, are discussed. Finally, the means of accurate estimation are proposed. Choosing the central region of flux linkage characteristics, adopting single-pulse operation throughout the speed range by means of voltage control, selecting appropriate phase for estimation, and introducing a correction factor 'Kc' (a function of voltage, speed and load) on static flux linkage, the sensorless operation is achieved. To implement the algorithm a* TMS320c50 DSP *platform is used. The controller was tested on a 5 hp 8/6* OULTON *motor. Results of tests, and accuracy of position estimate are presented. The accuracy of estimated position is found to be within ±1°. The proposed method uses only one phase voltage and one phase current for estimating the position.*

Keywords: *SR motor, flux linkage characteristics, estimation technique, eddy current effect, mutual inductance effect, voltage control.*

1. Introduction

Switched Reluctance (SR) Motor Drive has very good potential as an option for variable speed applications. Though simple in construction [1] and rugged, it needs accurate shaft position information for efficient control of the drive. A shaft encoder is usually employed for this purpose. But the presence of this shaft encoder increases the complexity and reduces the reliability of the drive. To obviate the position or speed sensors, this paper proposes a low-cost higher accuracy discrete position estimation method based on flux linkage characteristics of the SR motor.

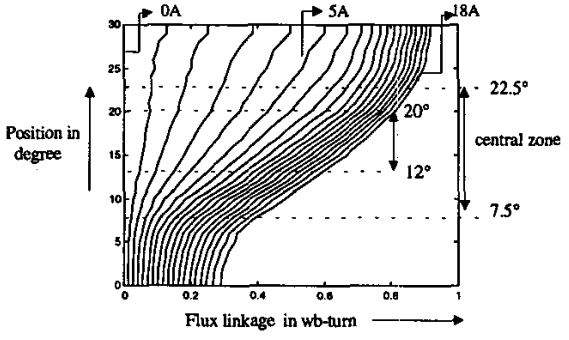

Fig. 1 Flux linkage Characteristics of a 4kw 8/6 SR motor

2.0 Position estimation

A number of methods have been proposed to do away with the position sensors. Detailed reviews of several schemes exist in the literature [1, 3-7]. Among these, the Flux-Current method [4, 5] is one of the most popular for obviating the need for sensors.

Typical magnetic characteristics of an SR motor are shown in Fig. 1 as rotor position vs flux linkage curves with current as a parameter. In the figure the unaligned position is shown as 0° and aligned position as 30°. For a given machine these characteristics are predetermined. Using this set value, the position of the shaft can be calculated by measuring the motor current and the flux linkage. The current can be measured by using a suitable current sensor, and the flux linkage Ψ is estimated from the equation

$$\Psi = \int (V - Ri)dt \qquad (1)$$

Though this method 'looks' very simple, getting the accurate magnetic characteristic is a good deal complex. Inaccuracy may result from instrumental and human error as well as from any discrepancy between the static and the dynamic characteristics of the motor [4]. A closer look at the flux linkage characteristics (Fig. 1) and a systematic study of the dynamic behaviour can lead to methods which will reduce the error substantially.

3.0 Sources of error

i) Eddy effect

The difference between the dynamic and the static characteristics of the magnetic circuit is mainly due to the rate of change of the flux in the magnetic circuit, which induces eddy currents in the coupled conducting paths. In static measurement [1, 2], since the rate of rise of current varies with the supply voltage, variations in the latter induce eddy currents. In static condition the flux linkage at 18° is measured using different voltages and the results are shown in Fig. 2. The test results show that the flux linkage changes with the excitation voltage. For a particular current the flux-linkage is reduced at higher voltages compared to that of at lower voltages. It proves that eddy effect is more at higher voltages and thus it reduces the net measured flux. The variation is found to be as high as

0-7803-4879-6/98/$10.00 © 1998 IEEE

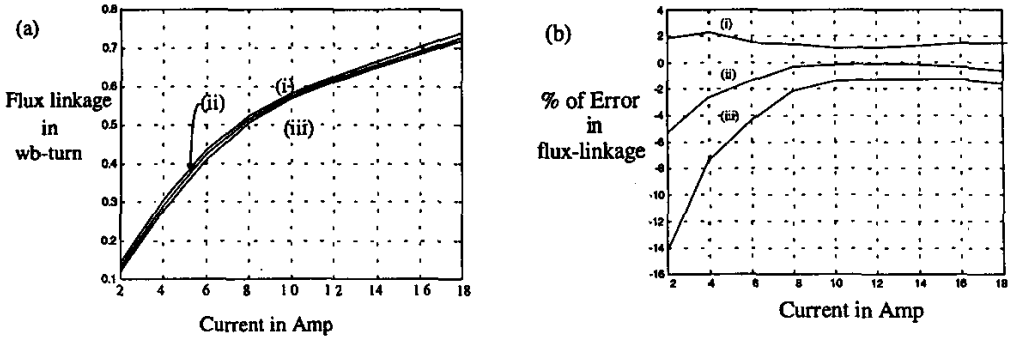

Fig. 2 The effect of excitation voltages on flux-linkage characteristics at 18°: (a) Flux and (b)% of difference in flux (with respect to the measured flux at 18°, with 60v as excitation voltage) for (i) 40v, (ii) 140v and (iii) 280v.

16% (Fig. 2(b)). In the case of a dynamic model, the rate of change of the flux depends on the position and speed of the rotor in addition to the nature of the current. From Fig.1 and Fig. 3, it can be seen that even if the current remains constant through the phase, the flux may vary due to changes in the rotor position and the rate of change of flux will be proportional to the speed (c.f. Eqn 2). So, there will be eddy effects even for a constant-current operation. Thus the eddy current effects lead to the discrepancy between the static and the dynamic flux linkages on account of voltage, speed and load currents.

ii) Mutual inductance effect

Another potential source of error in dynamic flux measurement is the mutual coupling effect induced by other current-carrying phases. In static flux measurements, only one phase is excited, and other phases are kept open [1,2], obviating mutual inductance effects. In dynamic cases, two, three or four phases may carry current simultaneously, and the flux linkage of each phase will be affected by all the other conducting phases. Fig. 4 shows the cross section of an 8/6 SR motor. The arrows in the figure indicates the direction of fluxes in individual poles when that particular phase is excited. It can be observed that mutual flux due to other phases have considerable influence on flux linkage characteristics of each of the phases. Fig. 5 shows the pictorial view of the mutual flux paths of Ph1 with its neighbouring phases (Ph4 and Ph2) The flux paths are shown in dotted lines. When Ph1 is at 0° (Fig. 5a) the mutual linkage to both the phases are equal. At 22.5° (Fig. 5b) the mutual flux between Ph1 and Ph4 will be maximum as the air-gap between the stator and the rotor along the flux path is minimum at that position. Similarly, at 37.5° (Fig. 5c) the mutual flux between the Ph1 and Ph2 is maximum. The mutual flux at other angular positions will take the intermediate values. The direction of the mutual fluxes (Figs. 5a, 5b and 5c) and the direction of self fluxes (Fig. 4) suggest that the mutual flux in Ph1 due to Ph4 will add to its own flux, whereas the mutual flux due to Ph2 will oppose it. An experiment is conducted to verify the nature and measure the magnitude of mutual fluxes of each phase. The details of the experiment is explained below.

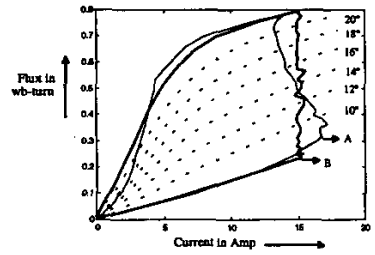

Fig. 3: Energy-conversion loop (Simulation result) at 450 rpm and full load: A in Single- Pulse mode (thin line), B in Chopping mode (bold line); Dotted curves are flux linkage characteristics between 10° and 20°.

3.1 Measurement of Mutual Flux:

Mutual flux -linkages in the neighbouring phases are measured when a particular phase is excited. The rotor is held standstill at a fixed position and a particular phase is excited for about 40 ms while the other phases are kept open. The current waveform in the activated phase and the induced voltages in the neighbouring phases are recorded on a DSO (Digital Storage Oscilloscope) and mutual flux to the neighbouring phases are computed off-line by integrating the induced voltage in those phases. The test is repeated for different positions. The test results are presented in Fig. 6. The test results show that though the mutual flux is one order less than the actual flux, still it can introduce an error of around 10% to the active phase and obviously that will influence the estimation method. All the angles referred in Fig. 6 correspond to the relative position of the rotor pole with respect to the phase being excited and are meant for the forward rotation of the motor (the arrows in Fig. 4 and Fig. 5 indicate the forward rotation). At 22.5° the mutual flux with the preceding phase is found to be the maximum. Similarly, when it is at 37.5° the mutual flux with the following phase is at maximum. This is in conformity with the earlier comments. Also the test results reveal that the mutual flux linkage of Ph1 with Ph2 is in opposite direction to

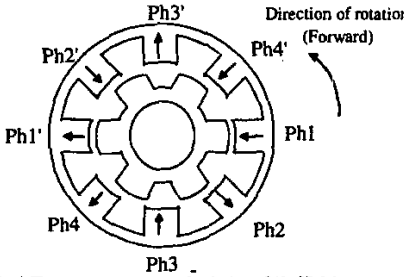

Fig.4 Flux pattern at poles of a 4 phase 8/6 SR Motor

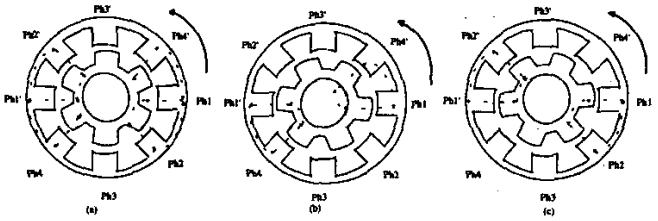

Fig. 5 Mutual Flux-linkages to its neighbouring phases when Ph1 is excited: (a) Ph1 is at 0°, (b) Ph1 at 22.5°, (c) Ph1 is at 37.5°

that of Ph1 with Ph4. Whereas the linkages on Ph3 due to Ph2 and Ph4 are in the same direction. This implies that when Ph4 and Ph2 both carry currents then the effect of their mutual flux to Ph1 will oppose each other and net mutual flux on Ph1 will be less. On the other hand, the mutual flux on Ph3 will be higher because both Ph2 and Ph4 mutual flux will add to each other at Ph3. The mutual flux due to Ph4 and Ph2 to their neighbouring phases are not shown, but their magnitude and nature are observed to be almost same as that of Ph1 and Ph3, and the directions are in conformity with Fig. 4. Thus it can be concluded that the error due to mutual fluxes on Ph1 and Ph4 fluxes will be less compared to that of Ph2 and Ph3.

3.2 Minimisation of error

Any error in the measurement of flux using the Flux-Current method under the sensorless scheme will give inaccurate information about position. So this method requires a good strategy to reduce the possibility of errors. We propose the following measures.

i) The central region of flux linkage characteristics

Figure 1 yields two observations. (1) Near the unaligned region, (θ close to 0°), the curves are vertical and very close; and (2) near the aligned region (θ close to 30°), the curves are almost vertical and thus susceptible to large errors if used for position estimation. From the plot, it can be ascertained that the region from 7.5° to 22.5° (central zone) is less susceptible to error than the extremities. The 12-20° region is recommended for more reasonable accuracy in position estimates.

But one distinct disadvantage of this zone (specially at high speeds) is that the mutual coupling effects here are more compared to the rest of the zone (c.f. Fig. 6a and 6b). For a 4-phase 8/6 motor the phase difference between the consecutive phases is 15°. So, when the active phase is within this zone the preceding phase will be within 27-35° region. For high speed operation there may be considerable current in the preceding phase during that period (c.f. Fig. 7), which will obviously influence the flux-linkage of the main phase due to the relatively higher mutual couplings. The phase following the main phase, remaining either in negative inductance region or near unaligned region (-3 to +5°), though having lower mutual coupling (due to higher air gap), will carry very high current (for high speed even it may carry more current than the main phase, c.f. Fig. 7). Due to this high current still this phase also may have some influence on the main flux. This mutual flux obviously will produce some error in the sensorless operation. This error can be minimised by choosing appropriate phase for estimation.

ii) Choosing appropriate phase for estimation

It is discussed in section 3.1 that the flux linkage of Ph1 and Ph4 suffer minimum error on account of mutuality. On the other hand, mutual effect on Ph2 and Ph3 are more. To illustrate this fact a simulation test is conducted and the typical results for the rated speed and full load are shown in Fig. 7. The result shows that near the commutation point (22.5 degree for this operating point) the mutual flux linkage to Ph2 and Ph3 are higher and positive, whereas they are close to zero for Ph1 and Ph4. So, it may appear that Ph1 and Ph4 will give better result in terms of position

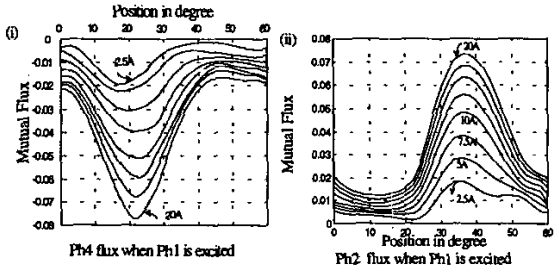

Fig. 6a. Mutual Flux -linkages of (i) Ph4 and (ii) Ph2 for the different excitation currents (2.5:2.5:20A) in Ph1.

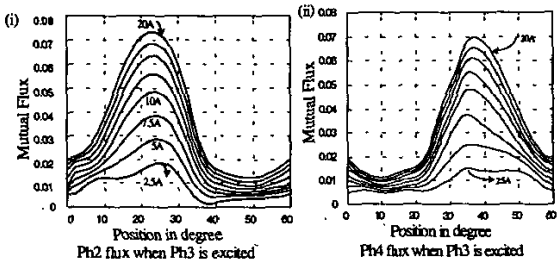

Fig. 6b. Mutual Flux -linkage of (i) Ph4 and (ii) Ph2 for the different excitation currents (2.5:2.5:20A)

estimation compared to Ph2 and Ph3. But in reality apart from mutual fluxes the other sources of error like eddy effect will be predominant. While on excitation, the eddy effects always oppose the main flux. The additional positive flux due to mutual coupling in Ph2 and Ph3 thus may get neutralised by the eddy effect and net error in position estimate may come down. Whereas for Ph1 and Ph4, the mutual inductance effect being minimum and the error due to eddy effect remaining uncompensated the net error in estimation may be more.

In section 3.2 (*i*), it is explained that during the central zone the mutual coupling of the main phase to the previous phase is more compared to the following phase and that can be viewed in Fig. 5 and Fig. 6. While in forward rotation the sequence of excitation for the different phases will be as Ph1-Ph2-Ph3-Ph4-Ph1. During the cntral zone if Ph1 is considered, the mutual flux due to Ph4 is negative and mutal flux due to Ph2 is positive. Since the mutual flux due to Ph4 is predominant compared to Ph2, therefore the resultant mutual flux on Ph1 is negative (c.f. Fig. 7). The negative effect of eddy current will be added to this net mutual flux in Ph1 and the net error may go up following this explanation. While for Ph4 the major contribution of the mutual flux will come from Ph3 and which is in the same direction of the main flux in Ph4 and thus the net mutual flux will be slightly positive for this case and that may reduce the net error marginally by neutralising the eddy effect.

So, it can be concluded that for forward rotation Ph2 and Ph3 are the best choices, followed by Ph4 and Ph1. Similarly, for reverse rotation also Ph2 and Ph3 retain the advantage over Ph1 and Ph4, but Ph1 gives marginally better results compared to Ph4.

iii) Current waveform: single pulse type

In a conventional SR motor drive, the motor is run in single-pulse mode only during high-speed operation. In this mode, the phase current rises sharply at the beginning, and falls gradually during the rest of the on-time. The relationship between voltage and current is given by Eq. 2.

$$v = Ri + \frac{\partial \Psi}{\partial \theta}\frac{d\theta}{dt} + \frac{\partial \Psi}{\partial i}\frac{di}{dt} \qquad (2)$$

In Eq.2 $\frac{\partial \Psi}{\partial \theta}\frac{d\theta}{dt}$ represents the back-emf. From Eq. 2, it can be shown analytically that the current through the winding can be kept almost constant throughout the central zone, if the applied voltage is made comparable to the back-emf.

In single-pulse operation the typical nature of the current waveform helps reduce the eddy effect in the central zone. Figure 4 shows the results of a simulation of the typical energy conversion loops for single-pulse operation (Trace A) and for chopping (Trace B). The

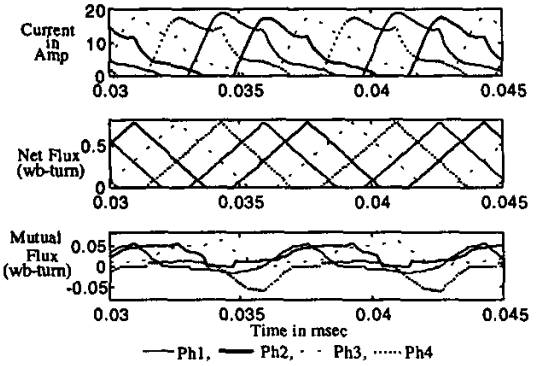

Fig. 7 Simulation result of Current (upper trace), Net Flux (middle trace) and Mutual Flux (lower trace) waveforms for all the phases at rated speed (1500 rpm) and full load (25 Nm).

two loops are considered for the same operating point (450 rpm and full load). In the case of single-pulse operation (trace A), though the current droops gradually in the central zone, the rate of change of flux, $\frac{d\Psi}{dt}$ (which is equivalent to $\frac{d\Psi}{d\theta}$ here, as the speed is constant), is less than that in the corresponding chopping mode. Thus it can be argued that in the central zone, the eddy effects are less in the single-pulse mode than in the chopping mode. The same logic can be applied throughout the speed range if the supply voltage is made a function of speed.

In the method proposed, a chopper circuit is incorporated between the rectifier and the power converter of the SR motor [8]. Thus the motor is supplied with a variable voltage. This variable voltage is made a function of speed so that it is capable of maintaining sufficient current in the presence of the back emf. In such a method, the machine is controlled in single-pulse mode, which makes it eminently suited to sensorless operation.

iv) Correction factor :function of voltage and load

It is already explained in section 3.0 that the eddy current is a function of excitation voltage, speed and load. In this particular control algorithm, voltage is made a function of speed so that the eddy effects can be expressed as a function of voltage (or speed) and phase current. Based on these observations, a correction factor 'Kc' is introduced here which is a function of supply voltage and phase current. For static measurements the supply voltage used, was 60V. So, to make the dynamic flux in conformity with the static flux the dynamic flux must be multiplied with a factor 'Kc'. For DC bus voltages of more than 60V, Kc >1. For lower voltages, Kc is less than one. For the test motor, Kc for Ph3 is observed to vary from 0.9 to 1.15.

4.0 Discrete and Continuous Estimation

The proposed method can be used for both continuous and discrete position estimation purposes.

In continuous position estimation, the flux linkage is computed for each of the phases. This method of continuous estimation of position requires more hardware for current and voltage sensing. Its execution time will also be more because of the increased number of analog inputs and the enhanced computation. Such expensive position estimators [7] may be justified only in a few critical applications such as servocontrol. In discrete position estimation (once in every cycle of 60° as in our case) the transient performance of the drive will be limited. But for cost-sensitive applications, still it is attractive [4, 5]. In this method, the reference angle must be chosen in such a way that an excitation current exists in the particular phase at this position even at very small loads. In this work, for discrete estimation the reference angle is chosen to be 18.75°. For continuous estimation, position may be estimated for each phase between 7.5° to 22.5°. Here, the correction factor 'Kc' will have to be different for different phases.

5.0 Algorithm for position estimation:

The current and voltage of a particular phase are monitored and the flux-linkage for that particular phase is calculated (at each instant). From the known values of current and flux linkage, position is obtained through a previously stored two dimensional look up table (which represents $\theta = f(i, \Psi)$). For a discrete method, searching of the look up table need not be continuous. Instead searching is restricted within the central zone (12° to 20°) around the reference angle (18.75°). The time at which the rotor position reaches the next central zone is roughly predicted from the knowledge of the previous position and speed of the motor, and a value corresponding to that time is loaded in a down counter. When this down counter counts down to zero, look up table searching is started. The instant at which the measured angle exceeds the reference (18.75° here), the absolute position of Ph3 is known (18.75°) and then the same process is repeated. Once the position of Ph3 is known the position of other phases can be obtained from the geometry of the motor (the displacement between the phases are 15^0).

5.1 Starting:

For sensorless operation of SR motor starting is not very straight forward. One phase sensing is not adequate for starting. In this paper starting is implemented through multiple phase sensing and once the motor has started, the operation is switched to single phase sensing for discrete estimation.

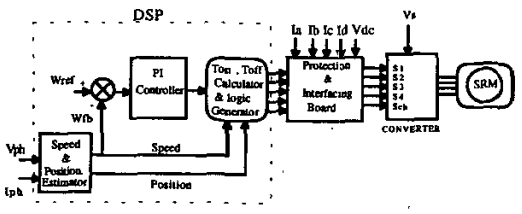

Fig.8 Block Diagram of the Proposed Controller

6.0 Realisation of the control algorithm

A TMS320c5x-based DSP-board is used for the implementation of the algorithm proposed here. The proposed algorithm needs only two items of information from the motor, viz., the current through and the voltage across Ph3. These analog signals are fed to the DSP through two simultaneously sampling ADCs. These signals are processed by the DSP, and the DSP provides five switching signals, one for each of the four phases of the motor, and one switching signal for the DC chopper switch control through a digital I/O port. The total control including speed and position information deduction, choosing appropriate T-on and T-off angles, control of chopper duty cycle etc. is effected by the DSP. The total control block diagram is shown in Fig. 8. The voltage control method is explained elaborately in [8].

7.0 Results

Using the estimated position through the proposed method the motor is run in the whole speed range and the performance is found to be satisfactory. Typical results of position estimation are shown in Fig. 9. The actual position is derived from the optical sensors mounted on the shaft of the motor. Whenever the rotor reaches the reference point (i.e. 18.75°) the optical sensor gives a high to low signal. In synchronism with that falling edge a counter (say counter1) gets set and starts upcounting till the next reference position is reached. Similarly, when the estimated position becomes 18.75°, another counter (say counter2) is set on. These two counts represent the relative position of the rotor with respect to the reference angle. The count values of the two counters are converted to the equivalent relative angles (with respect to the reference) and are plotted with respect to time (c.f. Fig 9). Both the counters are clocked at 50 μs. Position estimation algorithm is implemented using Ph1 and Ph3 separately. The plots (i), (ii) and (iii) in Fig. 9, are obtained without introducing any correction factor 'Kc' and using Ph1 for the estimation. The error margin for this experiment is found to be around $\pm 4^o$. Considering Ph3 for estimation and without using 'Kc' the error margin improves by almost 50% (i.e. the estimation error is within $\pm 2^o$, the results for which is not shown here due to limited space). The same estimation technique is implemented using Ph3 and considering the 'Kc'. The results for this test are shown in Fig. 9 (iv), (v) and (vi) for the same operating points as before. It can be seen that the improvement of error margin is quite impressive and the plots show that the error between the actual position of the motor and the position estimated by the scheme proposed is quite low (always within $\pm$ 1°). This error margin is quite acceptable in most of the cost critical applications like household appliances.

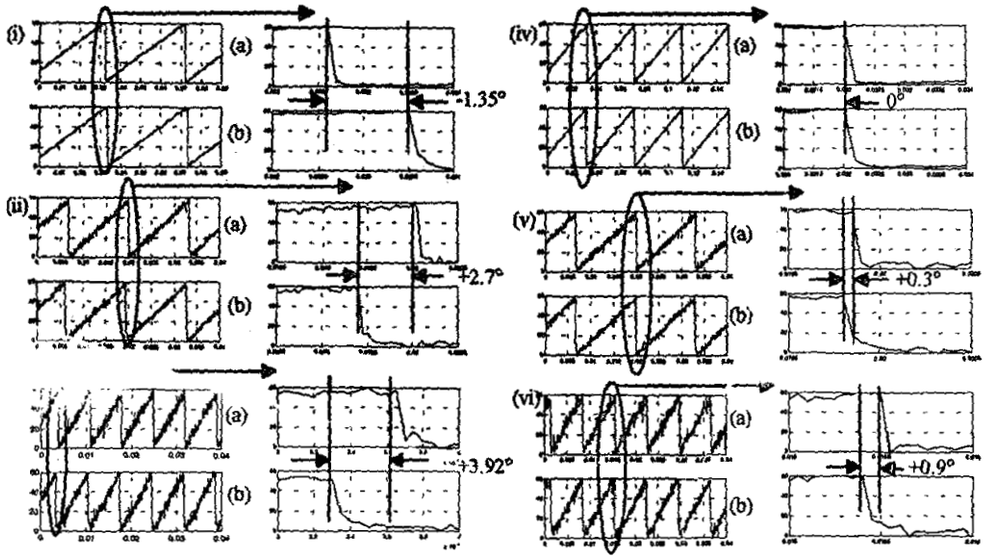

Fig 9 (a) Estimated Position and (b) Actual position for the following conditions: (i) at 250 rpm, (ii) at 750 rpm and (iii) at 1500 rpm without using the correction factor 'Kc' and using Ph1 for estimation; and (iv) at 250 rpm, (v) at 750 rpm and (vi) at 1500 rpm with correction factor 'Kc' and estimating the position by sensing Ph3. X-axis represents time in seconds and Y-axis represents position in degree. The enlarged view on the right of each figure show the error in degrees (error is the product of the time difference between the falling edges and speed).

8.0 Conclusion:

The algorithm proposed here uses only one phase current and one phase voltage for estimating the position. Voltage control method enables the operation of the motor in single pulse mode throughout the speed range, which makes the same estimation method effective for both low speed and high speed operations. The proposed method is least affected by the different non- idealities like eddy current and mutual inductances and that is verified through experimental results. This scheme of estimation is computationally simple and cost-effective. It requires a DSP platform with two ADCs and an 8-bit I/O port. This can be claimed as the minimum hardware requirement for any sensorless scheme of SR motor drive. The limitation of the scheme is that during starting it needs to sense multiple phase currents. So, the simplicity of single phase sensing is lost during starting. But the achievement of the proposed method in accuracy of position estimation is highly encouraging. The present scheme can be utilised in household appliances like washing machines, mixers, grinders and vacuum cleaners.

9.0 References:

1. Miller T.J.E.,"Switched Reluctance Motors and Their Control", Magna Physics Publishing And Clarendon Press Oxford 1993.
2. V. Ramanarayanan, L. Venkatesha, D. Panda, "Flux-linkage Characteristic of Switched Reluctance Motor", Power Electronics Drives and Energy System conference(PEDES-96) Delhi, December 1996, pp 281-285.
3. W. F. Ray and I. H. Al-bahadly, "Sensorless Methods for Determining the Rotor Position of Switched Reluctance Motor", Proc. of 5th Europeon Conference on Power Electronics and Applications, IEE publication no. 377, Sept. 93, Vol.6, pp 7-13.
4. J. P. Lyons, S. R. Macmin, M. A. Preston, "Flux/Current Method for SRM rotor position estimation", IEEE-Industry Application Society Annual Meeting, 1991, Vol.1, pp. 482-487.
5. W.F. Ray, I.H. Bahadly, "A sensorless method for Determining Rotor Position for Switched Reluctance Motor" Power Electronics and Variable speed drives conference publication no. 399,IEE, Oct. 1994, pp 13-17.
6. W.D. Harris and J.H.Lang,"A Simple Motion Estimator for Variable Reluctance Motors", IEEE Tr. on Industry Application, Vol. 26, No.2, March/April 1990, pp 237-243.
7. Acarnley P, French E.D. and Al-Bahadly I.H., "Position Estimation in Switched Reluctance Drives", Proc EPE'95, Seville, Vol 3, pp 765-770.
8. Debiprasad Panda and V. Ramanarayanan," Low-Noise Switched Reluctance Drive", IEEE conference PEDES'98.